

Fabrication and characterization of a composite dosimeter based on natural alexandrite



Neilo Marcos Trindade^{a,b,*}, Anna Luiza Metidieri Cruz Malthez^c, Augusto de Castro Nascimento^a, Ronaldo Santos da Silva^d, Luiz Gustavo Jacobsohn^b, Elisabeth Mateus Yoshimura^e

^a Federal Institute of Education, Science and Technology of São Paulo, Department of Physics, São Paulo, SP, Brazil

^b Clemson University, Department of Materials Science and Engineering, Clemson, SC, USA

^c Federal University of Technology – Paraná, Curitiba, PR, Brazil

^d Federal University of Sergipe, São Cristóvão, SE, Brazil

^e University of São Paulo, Institute of Physics, São Paulo, SP, Brazil

ARTICLE INFO

Keywords:
Alexandrite
OSL
Natural dosimeter
Mechanical properties

ABSTRACT

This work aims at demonstrating the fabrication of a new composite material based on the micron-sized powder of the alexandrite mineral ($\text{BeAl}_2\text{O}_4:\text{Cr}^{3+}$) dispersed in a fluorinated polymer for OSL dosimetric applications. Composites with 50 wt% alexandrite powders were obtained and characterized in their chemical composition, mechanical, and luminescent properties. Energy dispersive X-ray spectroscopy mapping measurements of the pellets revealed a homogeneous distribution of alexandrite particles throughout the organic matrix. PL measurements showed the signal related to Cr^{3+} ions in alexandrite remained active besides all fabrication steps, and tensile tests showed the pellets to have good ductility and tensile strength. The OSL results showed the integrated intensity signal varied linearly with the beta irradiation dose and that the pellets were stable at room temperature over time of 28 days. Nevertheless, improvements in the fabrication process are necessary toward obtaining the same OSL intensity from different pellets.

1. Introduction

Natural and synthetic dosimetric materials are used for the determination of the irradiation dose received in the environment as well as in medical and technological activities. Synthetic dosimeters have the advantage of controlled synthesis and precise chemical composition thus presenting high levels of reproducibility. On the other hand, natural dosimeters find application, *e.g.*, in retrospective dosimetry and may be a lower-cost alternative to synthetic ones. Further, they may be more readily available in large quantities [1].

Optically stimulated luminescence (OSL) has long established itself as a reliable technique in dosimetry. The OSL signal arises from the recombination of charges optically released from specific traps inside the material that was previously irradiated with ionizing radiation. The charge carrier population in the traps is the result of the irradiation, and thus the OSL intensity is related to the absorbed radiation dose [2–4]. The OSL signal obtained under stimulation with constant light power is observed to progressively decrease as the charges are released from the traps (decay curve) [3]. Due to the optical nature of the process, the OSL technique presents several advantages such as simplicity of

measurement, possibility of reevaluation of irradiation doses, and flexibility for obtaining cumulated and individual dose measurements with the same detector [4,5]. Since the OSL signal can be monitored at room temperature without heating the material, the readout process is less destructive and usually does not affect the defects involved in the luminescence mechanism. On the other hand, the main disadvantage of this technique lies in the low number of materials that present intrinsic characteristics suitable for application in radiation dosimetry [4,6]. Therefore, due to the advantages of the OSL technique and the low number of commercially available OSL detectors, there is need to discover and develop new OSL dosimetric materials [7–10]. In terms of natural dosimetric materials, this effort has been mostly directed to accident dosimetry and luminescence dating [3] using quartz and feldspar.

The material under consideration in this work is the mineral alexandrite ($\text{BeAl}_2\text{O}_4:\text{Cr}^{3+}$), with the largest deposits in the world found in the Brazilian States of Bahia, Espírito Santo, and Minas Gerais [11]. Alexandrite, a variety of the mineral Chrysoberyl, has a fraction of its Al ions substituted by Cr ions and thus its unique optical properties. Chrysoberyl has a closed hexagonal (hcp) structure and the unit cell

* Corresponding author. Federal Institute of Education, Science and Technology of São Paulo, Department of Physics, São Paulo, SP, Brazil.
E-mail address: ntrindade@ifsp.edu.br (N.M. Trindade).

contains four formula units ($Z = 4$). Eight Al^{3+} ions occupy distorted octahedral sites and four Be^{2+} ions occupy distorted tetrahedral sites. The distortion in the hcp structure gives rise to the appearance of two distinct crystallographic sites: Al_1 , located at inversion sites, and Al_2 located at a reflection plane [12,13]. The larger Cr^{3+} ions are preferably incorporated into the larger Al_2 site that has an average $\text{Al}-\text{O}$ bond length of 1.938 \AA , instead of the Al_1 site with an average $\text{Al}-\text{O}$ bond length of 1.890 \AA [14,15]. According to the literature, Cr^{3+} ions located in the Al_2 sites are responsible for the optical properties of alexandrite, including laser emission [14,16–18].

The motivation for this work lies on the fact that chrysoberyls contain 19.8 wt% BeO and 80.2 wt% Al_2O_3 [19] with both of these simple oxides being commercially used as OSL dosimeters. $\text{Al}_2\text{O}_3:\text{C}$, first developed as a highly sensitive TL material [20], became widely used as an OSL sensor because of its thermal stability close to room temperature, reproducibility, sensitivity to low gamma-ray irradiation doses down to $1 \mu\text{Gy}$, low fading rate ($< 5\%$ per year), and the capability for imaging radiation fields [21]. BeO was suggested as an OSL dosimeter in the 1970s [22], but its properties were only investigated in detail in the late 1990s [23]. This dosimeter has been used in photon and beta dosimetry [24] combined with being a low-cost material [25]. BeO presents high sensitivity to ionization radiation, linear dose response in a broad range from $1 \mu\text{Gy}$ to 5 Gy [21], and negligible fading within long storage times ($< 1\%$ in 6 months) [25]. The low effective atomic number ($Z_{\text{eff}} = 7.14$ [26]; 7.21 [21]) of BeO is near tissue-equivalent and allows for medical applications [26].

The investigation of the potential of alexandrite as a dosimetric material was executed by means of thermoluminescence measurements and first reported in Ref. [27]. This paper focuses on the development and the characterization of a dosimetric composite based on the powdered mineral dispersed in a binder, a fluorinated polymer, toward achieving higher control and reproducibility of the dosimetric response. The dosimetric properties of this new dosimetric composite are reported here for the first time.

2. Materials and methods

2.1. Preparation of powdered alexandrite

The natural sample used in this work was originated from the State of Bahia, Brazil. The procedure for obtaining alexandrite powder was as follows:

1. Crystals of green alexandrite were visually separated from the natural piece of rock.
2. These fragments were manually crushed and powdered using a Chiarotti porcelain mortar and pestle.
3. The powder was sieved with a pair of Granutest sieves, selecting grain sizes smaller than $75 \mu\text{m}$.
4. The sieved alexandrite powder was thermally treated at 400°C for 1 h to clean any signal previously accumulated in the material due to natural irradiation.

2.2. Preparation of alexandrite composite pellets

The composite pellets were obtained using a proprietary technique for OSL sheet production developed at the Federal University of Technology in Curitiba, Paraná, Brazil. The fabrication process consisted in mixing the alexandrite powder with an organic matrix based on a fluorinated polymer on a 1:1 mass ratio. This matrix was chosen to embed the alexandrite powder because it does not emit any OSL signal, and because it gives rise to a good sheet homogeneity. Finally, 1.4 mm thick, 5.5 mm diameter, and 1.87 g/cm^3 average density pellets were obtained from the original sheet using a handheld slot punch.

2.3. Characterization of alexandrite pellets

The surface morphology and microstructure of the samples were imaged by means of scanning electron microscopy (SEM) measurements in backscattered electron (BSE) mode, while the local chemical composition was determined by energy dispersive X-ray spectroscopy (EDS) measurements using a Hitachi S-3400 N scanning electron microscope.

Tensile strength test of the composite was executed using Instron 5500R1125 and 4582 tensile analyzers. The analysis was carried out at room temperature at a speed of 10 mm/min using a sample with a rectangular shape (6 mm length, 6.76 mm width, 1.45 mm thickness). From these measurements, the Young's modulus, maximum load, and elongation were determined using the Bluehill 2 Software.

Steady-state photoluminescence emission (PL) spectra were collected with a Horiba Jobin-Yvon Spex FluoroLog 2 spectrofluorometer equipped with a Hamamatsu R928 photomultiplier detector. The equipment has double monochromators for both excitation and detection, and a 450 W xenon lamp as the excitation source. The measurements were carried out at room temperature with a 2 nm excitation slit, 1 nm emission slit, 0.5 nm wavelength increment step, and 0.5 s integration time.

OSL measurements were carried out using a commercial automated TL/OSL reader produced by Risø National Laboratory (model DA-20). OSL luminescence was stimulated using blue light emitting diodes (470 nm, FWHM = 20 nm) delivering 80 mW/cm^2 at the sample position in CW mode. Each OSL measurement was carried out with 90% of the maximum LED power density. The OSL signal was detected with a bialkali photomultiplier tube (PMT) behind an UV transmitting broadband glass filter (Hoya U-340, 7.5 mm thick) to block the stimulation light while transmitting part of the OSL signal from the samples. Irradiation was performed at room temperature using the built-in ${}^{90}\text{Sr}/{}^{90}\text{Y}$ beta source of the TL/OSL reader (dose rate of 10 mGy/s) within a dose range from 100 to 500 mGy.

3. Results and discussion

Fig. 1 shows the as-received alexandrite mineral before any processing (a), the powder before sieving (b), the alexandrite: fluorinated polymer composite sheet (c), and the 5.5 mm diameter pellet (d). Fig. 2 shows a SEM image of the pellet surface (central image, top layer) while composition mapping of selected chemical elements (C, Mg, Al, Ca, Fe) are shown in the surrounding images. Visual analysis showed that each element presented a uniquely different distribution in the sample. Since Be cannot be detected by EDS, the distribution of alexandrite particles within the polymeric matrix was determined through the mapping of Al. These results indicated the alexandrite particles were reasonably well homogeneously distributed in the matrix. Fe is a common impurity of alexandrite and its distribution to regions rich in Al (*i.e.*, the alexandrite phase). Because of the low concentration, Cr was not detected in this experiment. In a previous work, we have shown that the natural mineral alexandrite contained other phases, including mica, allanite, and apatite [27]. These secondary phases were revealed through the presence and distribution of elements like Mg and Ca. Mg is commonly present in mica, and Ca is commonly found in apatite. As expected, the distribution of these elements did not match that of alexandrite (Al). C was originated from the polymeric matrix. Similar results were obtained from other pellets analyzed the same way. According to previous work on the same group of alexandrite samples, the Cr and Fe average concentration values are 0.7 wt% and 1.9 wt%, respectively [27]. As discussed before in the literature, Cr and Fe are responsible for the optical and luminescent properties [14,16,18, 27,28].

In order to evaluate some of the effects of handling of the composite, the mechanical response under tensile stress was investigated. A typical load/deformation curve is presented in Fig. 3. The results showed a significant plastic deformation and energy absorption (toughness) before the fracture, demonstrating the ductile nature of the composite

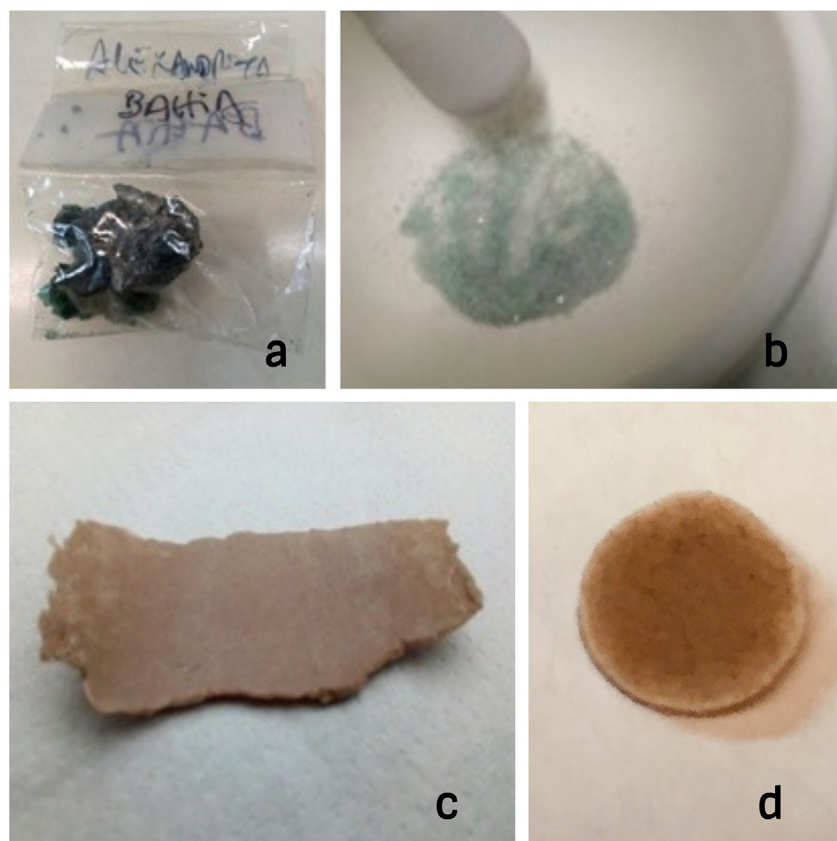


Fig. 1. a) The as-received alexandrite mineral before any processing, b) the powder before sieving, c) the alexandrite: fluorinated polymer composite sheet, and d) the 5.5 mm diameter pellet.

material. Other results from this analysis included the determination of the Young's modulus to be 0.25 MPa, maximum load of 5.97 N with true strain of 1.52, and 356% elongation. The shape of the load/deformation curve showed that there was no linearity between tension and deformation. This was tentatively explained by the crystallization of the polymer at large elongation values. The crystallization decreases the flexibility of the polymer molecules, restricting the deformation and requiring a higher than expected tension value. Consequently, the Young's modulus should be considered a combination of the moduli of

the crystalline and amorphous phases of the polymer [29]. In summary, these results showed the composite to exhibit good ductility and tensile strength.

The luminescent properties of the composite pellet were characterized by PL measurements excited at 420 nm, as shown in Fig. 4. These measurements were executed to verify if the fabrication steps affected the Cr^{3+} ions emission centers. The emission spectrum showed one narrow main line centered at 682 nm. This line was assigned to be the non-resolved superposition of the R lines commonly associated with

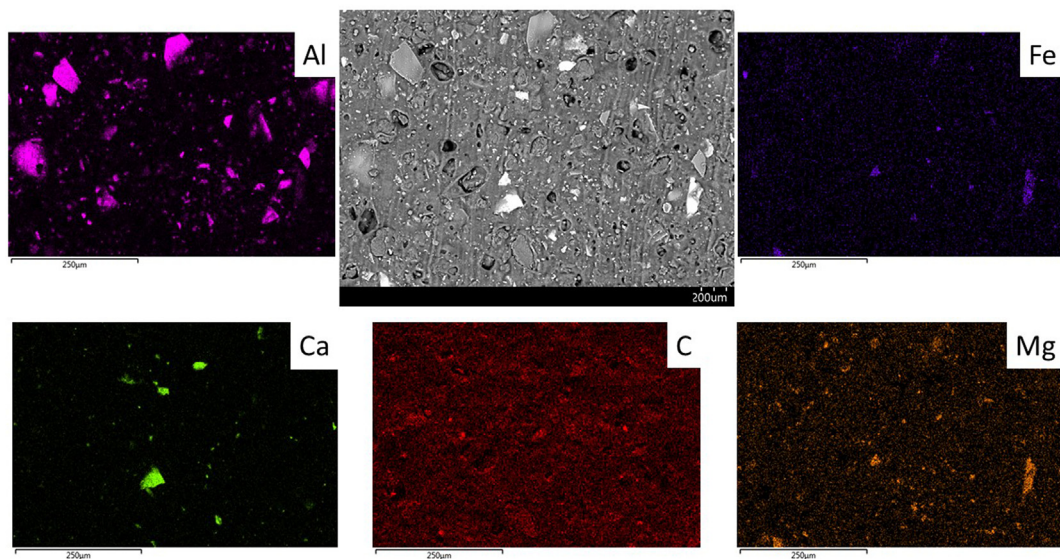


Fig. 2. SEM image of the pellet surface (central image, top layer) together with the mapping of selected chemical elements: C, Mg, Al, Ca, Fe (surrounding images).

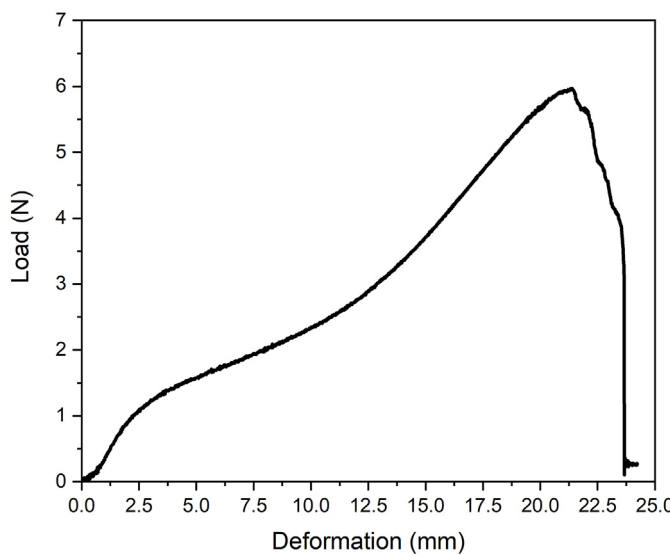


Fig. 3. Load/deformation curve of the composite sheet.

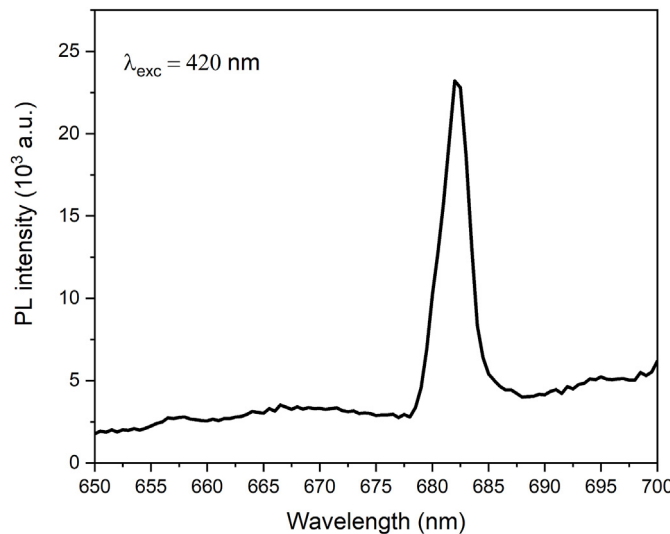


Fig. 4. Photoluminescence spectrum of a composite pellet obtained under excitation at 420 nm.

Cr^{3+} located at the Al_2 sites. In synthetic alexandrite single crystals, these lines are found at around 678 and 680 nm at room temperature [13,27,30–32], in reasonable agreement with the emission of the natural mineral. These results showed that alexandrite micro-sized powder dispersed in the polymer matrix continued to exhibit its luminescent properties.

Fig. 5a shows the original OSL decay curves for a pellet irradiated with different doses and results in semi-logarithmic scale are shown in the inset. This result showed all the decay curves can be described by the same decay function that linearly depends on the irradiation dose through the multiplicative constant. Fig. 5b shows normalized OSL decay curves obtained for the same sample. It was noted that the shape of the OSL decay curve was independent of the irradiation dose, an important characteristic for an OSL dosimetric material. It was also observed that the OSL response had fallen to less than 5% of the initial intensity in about 20 s of continuous light stimulation. Essentially all traps involved in the OSL process were emptied within 20 s of illumination with the power used in the experiment. Moreover, Fig. 6 shows the average of the integrated OLS intensity of six pellets as a function of the irradiation dose. The value of the OSL intensity was taken as the

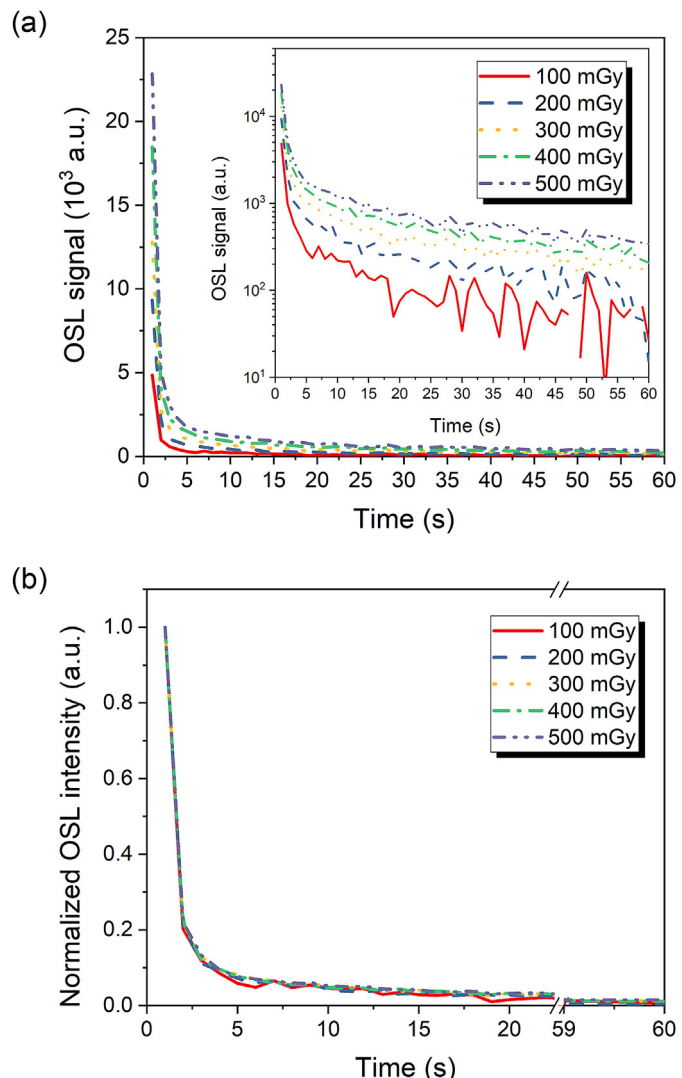


Fig. 5. a) Original OSL decay curves of a composite pellet obtained for different beta irradiation doses and results in semi-logarithmic scale in the inset; b) normalized OSL intensity decay curves for the same sample.

integral of the decay curve in the first 20 s after the subtraction of the background signal obtained from the integral of the curve in the 21–40 s time interval. The average integrated OSL signal increased linearly with the irradiation dose, as demonstrated by the linear best fit shown in the figure that achieved a regression coefficient of 0.997. For the same irradiation dose, the percentual standard deviation of the response of the six different pellets was about 7% in relation to the average value.

In order to test the reproducibility of the OSL signal, three OSL measurements were obtained from each of six different pellets irradiated up to 300 mGy. A 300 s illumination was carried before each OSL measurement to empty all traps. The integrated OSL intensity versus the measurement tag number is shown in Fig. 7 for each pellet. For each pellet, the OSL signal was found to be reproducible when re-measured under the same conditions. In fact, the coefficient of variance ($CV = \text{standard deviation}/\text{mean value}$) of each pellet did not exceed 5%, with pellet #1 having a CV as low as 0.65%. On the other hand, when comparing the results among the six different pellets, the CV rises to 17%. While further work is still necessary to fully understand the reasons for the response variation among different pellets, it was found that the mass of the pellets presented a variation of about 10% and thus a likely variation in the content of the mineral powder. Also, even if all

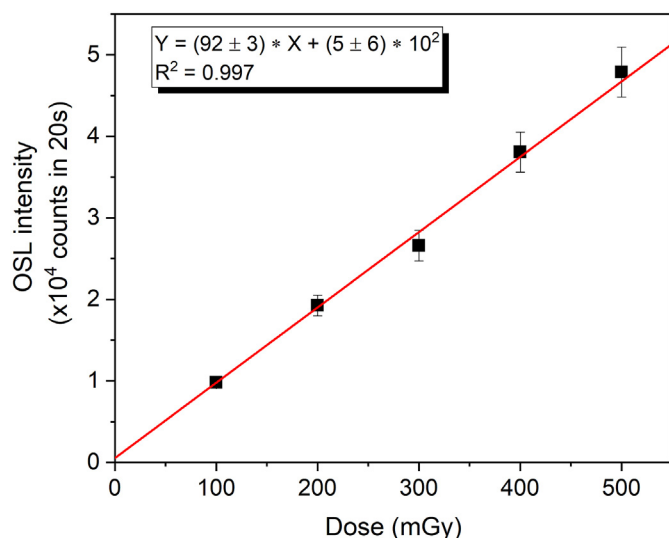


Fig. 6. Average OSL intensity from six different composite pellets as a function of the beta irradiation dose. The error bars correspond to the percentual standard deviation in relation to the average value. The red straight line corresponds to the linear best fit indicated in the box. (For interpretation of the references to colour in this figure legend, the reader is referred to the Web version of this article.)

pellets had the same mass of mineral powder, variations of the amount of the alexandrite phase are expected in a natural mineral.

Fading tests were performed for 3 different storage times in the dark using 3 different pellets. These results are summarized in Fig. 8 where the average intensity values normalized to the corresponding initial value obtained at $t = 0$ s and their respective standard deviations are shown as a function of storage time. While these results revealed a fast fading of about 20% within the first hour of storage, no further fading was observed over a period of 28 days with the pellets retaining about 80% of the initial signal.

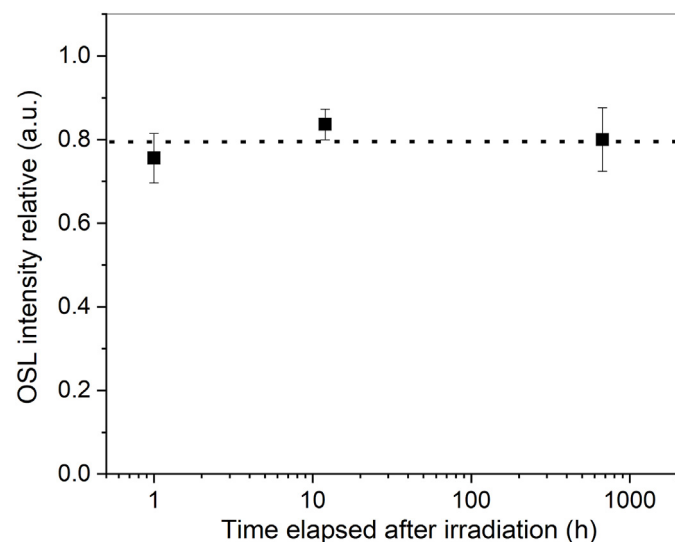


Fig. 8. Average integrated OSL intensity values normalized to the corresponding initial value obtained at $t = 0$ s and their respective standard deviations as a function of storage time.

4. Conclusions

This work aims at demonstrating the fabrication of a new composite material based on the micron-sized powder of the alexandrite mineral dispersed in a fluorinated polymer for OSL dosimetric applications. Composites with 50 wt% alexandrite powders were obtained and characterized in their chemical composition, mechanical, and luminescent properties. EDS mapping measurements of the pellets revealed a homogeneous distribution of alexandrite particles throughout the organic matrix, while PL measurements showed the signal related to Cr³⁺ ions in alexandrite remained active besides all fabrication steps. Also, the pellets showed good ductility and tensile strength. The OSL results showed important characteristics for dosimetry, including that the integrated intensity signal varied linearly with the beta irradiation dose, and that each pellet was stable at room temperature over long

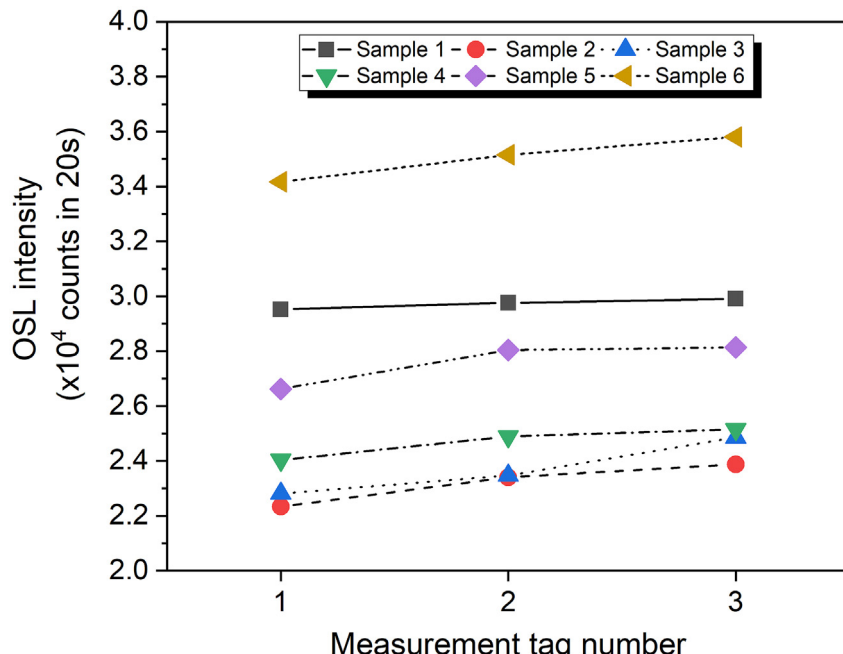


Fig. 7. Reproducibility evaluation of the OSL response: integrated OSL intensity of three OSL measurements obtained from six different pellets irradiated up to 300 mGy.

times (28 days). Nevertheless, improvements in the fabrication process are necessary toward obtaining the same OSL intensity from different pellets.

Acknowledgments

A.C. Nascimento is grateful for the scholarship received from the National Council for Scientific and Technological Development (CNPq), Brazil. E. M. Yoshimura acknowledges National Council for Scientific and Technological Development (CNPq), Brazil, Grant #307375/2015-3. Funding for this work was provided by the Brazilian agency São Paulo Research Foundation (FAPESP), Grant #2017/11663-1. This material is based upon work supported by the National Science Foundation, Grant #1653016.

References

- [1] D.N. Souza, M.E.G. Valerio, J.F. de Lima, L.V.E. Caldas, Nuclear Instruments and Methods in Physics Research Section B: Beam Interactions with Materials and Atoms vols. 166–167, (2000), pp. 209–214.
- [2] A.S. Pradhan, J.I. Lee, J.L. Kim, J. Med. Phys./Assoc. Med. Phys. India 33 (2008) 85–99.
- [3] L. Bøtter-Jensen, Development of Optically Stimulated Luminescence Techniques Using Natural Minerals and Ceramics, and Their Application to Retrospective Dosimetry, Nuclear Safety Research and Facilities Department, University of Copenhagen, Copenhagen, 2000, p. 185.
- [4] E.G. Yukihara, S.W.S. McKeever, Optically Stimulated Luminescence: Fundamentals and Applications, John Wiley and Sons, West Sussex, UK, 2011.
- [5] A.L.M.C. Malthez, M.B. Freitas, E.M. Yoshimura, V.L.S.N. Button, Radiat. Phys. Chem. 95 (2014) 134–136.
- [6] E.G. Yukihara, S.W.S. McKeever, Phys. Med. Biol. 53 (2008) R351.
- [7] E.G. Yukihara, E.D. Milliken, L.C. Oliveira, V.R. Orante-Barrón, L.G. Jacobsohn, M.W. Blair, J. Lumin. 133 (2013) 203–210.
- [8] J.R. Hazelton, E.G. Yukihara, L.G. Jacobsohn, M.W. Blair, R. Muenchhausen, Radiat. Meas. 45 (2010) 681–683.
- [9] M.W. Blair, L.G. Jacobsohn, S.C. Tornag, O. Ugurlu, B.L. Bennett, E.G. Yukihara, R.E. Muenchhausen, J. Lumin. 130 (2010) 825–831.
- [10] E.M. Yoshimura, E.G. Yukihara, Nuclear Instruments and Methods in Physics Research Section B: Beam Interactions with Materials and Atoms vol. 250, (2006), pp. 337–341.
- [11] M.S. Basilio, A. Pedrosa-Soares, H. Jordt-Evangelista, Revista Geonomos 8 (2000) 8.
- [12] B.K. Sevastyanov, Crystallogr. Rep. 48 (2003) 989–1011.
- [13] N.M. Trindade, A. Tabata, R.M.F. Scalvi, L.V.d.A. Scalvi, Mater. Sci. Appl. 2 (2011) 4.
- [14] S.-U. Weber, M. Grodzicki, W. Lottermoser, G.J. Redhammer, G. Tippelt, J. Ponahlo, G. Amthauer, Phys. Chem. Miner. 34 (2007) 507–515.
- [15] R.M.F. Scalvi, M.S. Li, L.V.A. Scalvi, Phys. Chem. Miner. 31 (2005) 733–737.
- [16] K.L. Schepler, J. Appl. Phys. 56 (1984) 1314–1318.
- [17] D.A. Vinnik, D.A. Zherebtsov, S.A. Archugov, M. Bischoff, R. Niewa, Cryst. Growth Des. 12 (2012) 3954–3956.
- [18] R.M.F. Scalvi, L. de Oliveira Ruggiero, M. Siu Li, Powder Diffr. 17 (2002) 135–138.
- [19] V.Y. Ivanov, V.A. Pustovarov, E.S. Shlygin, A.V. Korotaev, A.V. Kruzhakov, Phys. Solid State 47 (2005) 466–473.
- [20] M.S. Akselrod, V.S. Kortov, D.J. Kravetsky, V.I. Gotlib, Radiat. Protect. Dosim. 33 (1990) 119–122.
- [21] M.S. Akselrod, AIP Conference Proceedings 1345 (2011) 274–302.
- [22] C.R. Rhyner, W.G. Miller, Health Phys. 18 (1970) 681–684.
- [23] E. Bulur, H.Y. Göksu, Radiat. Meas. 29 (1998) 639–650.
- [24] A. Jahn, M. Sommer, J. Henniger, Radiat. Meas. 71 (2014) 104–107.
- [25] M. Sommer, J. Henniger, Radiat. Protect. Dosim. 119 (2006) 394–397.
- [26] M. Sommer, A. Jahn, J. Henniger, Radiat. Meas. 43 (2008) 353–356.
- [27] N.M. Trindade, H. Kahn, E.M. Yoshimura, J. Lumin. 195 (2018) 356–361.
- [28] N.M. Trindade, R.M.F. Scalvi, L.V.A. Scalvi, Energy Power Eng. 2 (2010) 7.
- [29] W.D. Callister, Materials Science and Engineering: an Introduction, seventh ed., John Wiley & Sons., New York, 2007.
- [30] N. Ollier, Y. Fuchs, O. Cavani, A.H. Horn, S. Rossano, Eur. J. Mineral 27 (2015) 783–792.
- [31] R.C. Powell, L. Xi, X. Gang, G.J. Quarles, J.C. Walling, Phys. Rev. B 32 (1985) 2788–2797.
- [32] A.B. Suchocki, G.D. Gilliland, R.C. Powell, J.M. Bowen, J.C. Walling, J. Lumin. 37 (1987) 29–37.